



# Electronic and magnetic properties of the $\text{Co}_2\text{MnAl}/\text{Au}$ interface: Relevance of the Heusler alloy termination



L. Makinistian<sup>a,b,\*</sup>, E.A. Albanesi<sup>a,b</sup>

<sup>a</sup> Instituto de Física del Litoral (CONICET-UNL), Güemes 3450, 3000 Santa Fe, Argentina

<sup>b</sup> Facultad de Ingeniería, Universidad Nacional de Entre Ríos, 3101 Oro Verde, Argentina

## ARTICLE INFO

### Article history:

Received 6 May 2014

Received in revised form

12 February 2015

Accepted 27 February 2015

Available online 2 March 2015

### Keywords:

Heusler alloys

N/F interfaces

Spintronics

## ABSTRACT

We present *ab initio* calculations of electronic and magnetic properties of the ferromagnetic metal/normal metal (F/N) interface of the Heusler alloy  $\text{Co}_2\text{MnAl}$  and gold. Two structural models are implemented: one with the ferromagnet slab terminated in a pure cobalt plane (“ $\text{Co}_2\text{-t}$ ”), and the other with it terminated with a plane of MnAl (“ $\text{MnAl-t}$ ”). The relaxed optimum distance between the slabs is determined for the two models before densities of states, magnetic moments, and the electric potential are resolved and analyzed layer by layer through the interface. Complementary, calculations for the free surfaces of gold and the Heusler alloy (for both models,  $\text{Co}_2\text{-t}$  and  $\text{MnAl-t}$ ) are performed for a better interpretation of the physics of the interface. We predict important differences between the two models, suggesting that both terminations are to be expected to display sensibly different spin injection performances.

© 2015 Elsevier B.V. All rights reserved.

## 1. Introduction

Heusler alloys have received a remarkable attention since the prediction by de Groot et al. [1,2] in the early 1980s that some of these compounds would have a 100% spin-polarization at the Fermi level [3–6]. Their high spin polarization and high Curie temperatures are advantageous for many possible applications in the field of spintronics [7,8]: from achieving high tunnel magneto-resistance (TMR) ratios in tunnel junctions to efficient spin injection from ferromagnetic electrodes into semiconductors. Heusler alloys are ternary intermetallic compounds with an  $\text{L}_{21}$  lattice structure (225-Fm3m space group), and an  $\text{X}_2\text{YZ}$  stoichiometry, where X can be a 3d, 4d, or 5d element (e.g., Co, Fe, Ni or Cu), Y can be, e.g., Ti, V, Cr, Mn or Fe, and Z can be, e.g., Al, Si, Ga, As, In, or Sn. They present layers of YZ atoms arranged in a plane square lattice alternated with layers of X atoms [9].

An important subset of the Heusler alloys are the ones based on cobalt ( $\text{Co}_2\text{YZ}$ ), which have been utilized in spintronic heterojunctions. For instance,  $\text{Co}_2\text{MnSi}$  was recently used as a magnetic electrode in magnetic tunnel junctions (MTJ) finding TMR ratios of 570% at 2 K, while  $\text{Co}_2\text{MnGe}$  as a spin injector into a p–i–n type emitting diode [10–12]. Regarding  $\text{Co}_2\text{MnAl}$ , experimental and theoretical studies can be found in the literature [3,13–20],

including its application in magneto-optical devices [21] or as a spin-injector (into p-type GaAs, with a higher performance than other Heusler alloys [22]). However, to the best of our knowledge the effects of its contact with a normal metal have not been reported to date: this being of key relevance in better understanding the behavior of devices that will typically involve normal-metallic electrodes (and/or a normal-metal spacer between ferromagnetic electrodes [23]), in this work we study the electronic and magnetic properties of its interface with gold.

## 2. Computational details

For the study of the  $\text{Co}_2\text{MnAl}/\text{Au}$  interface, we carried out calculations for seven separate systems: bulk  $\text{Co}_2\text{MnAl}$ , bulk Au, two different models for the interface and the corresponding two for the free surface, and the free surface of gold. Due to the layered structure of the Heusler alloy (alternating layers of  $\text{Co}_2$  and MnAl planar lattices), there are two possible configurations for an ideal (i.e., defects free) interface parallel to the plane (0 0 1): the gold can be in direct contact with a 2D square lattice of either  $\text{Co}_2$  (see Fig. 1(b)), or of MnAl (Fig. 1(c)). We will address the first as  $\text{Co}_2\text{-t}$ , and the latter as MnAl-t (as abbreviations for “ $\text{Co}_2$ -terminated interface” and “MnAl-terminated interface”, respectively). Figs. 1 (a) and (d) show the corresponding free surfaces, and Fig. 1 (e) shows the free surface of gold.

The experimental lattice parameter of  $\text{Co}_2\text{MnAl}$  is of 5.749 Å (Ref. [17]), and the lattice constant of gold equals 4.0786 Å so the

\* Corresponding author at: Instituto de Física del Litoral (CONICET-UNL), Güemes 3450, 3000 Santa Fe, Argentina.

E-mail address: [lmakinistian@santafe-conicet.gov.ar](mailto:lmakinistian@santafe-conicet.gov.ar) (L. Makinistian).

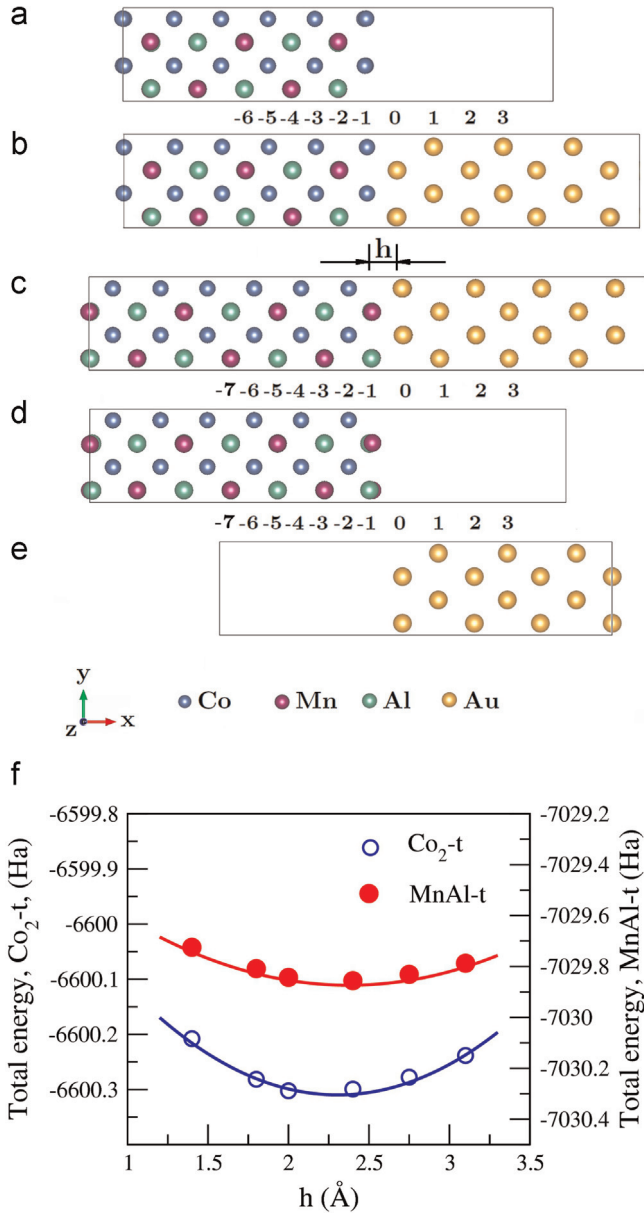


**Fig. 1.** Co<sub>2</sub>-terminated free surface (a) and interface (b), MnAl-terminated interface, (c) free surface (d), and free surface of gold (e); integers (–7...5) number the atomic layers for later reference. (f) Optimization of the interface separation,  $h$ , for both models. The optimum separations,  $h^0$ , are  $h_{\text{Co}_2\text{-t}}^0 = 2.31$  Å and  $h_{\text{MnAl-t}}^0 = 2.37$  Å.

diagonals of any of its unit cell's faces equal 5.7680 Å. To resolve the slight lattice mismatch (only  $\sim 0.33\%$ ) we used 5.7585 Å for the Heusler and 4.0719 Å for the gold lattice parameter and we rotated the gold lattice  $45^\circ$  around the  $[001]$  direction. For the Co<sub>2</sub>-t model (total of 72 atoms) we used 6 layers of Co intercalated with 5 of MnAl, while for the MnAl-t model (total of 80 atoms), we used 7 layers of MnAl (see Fig. 1); the gold slab (total of 28 atoms) was made of 7 layers. We tested the most central layers densities of states (DOS) against those of the bulk materials and found an excellent agreement, concluding that our slabs were thick enough to actually model the interface (instead of a superlattice with interacting interfaces). For the free surfaces, a vacuum slab of  $\sim 12$  Å was included in the supercell to avoid coupling due to the periodic conditions (e.g., Ref. [24]). For the discretization of real space we used a cutoff energy of 150 Ry and the four atomic layers closer to the interface plane, and the two closest to the free surface, were left to relax (leaving all the rest with their atomic positions fixed to

a maximum force of  $\sim 10^{-3}$  Ha/Bohr), using a  $1 \times 3 \times 3$  mesh in  $k$ -space for the interfaces and of  $1 \times 9 \times 9$  for the free surfaces. All electronic densities, densities of states (DOS) and electric potential were calculated with a  $1 \times 9 \times 9$  mesh, which proved to produce DOS's of the bulk-like layers (–7, –6, –5, –4, and 3, see Fig. 1) in excellent agreement with those of the pure, bulk materials. We considered only collinear magnetism, i.e., spin-orbit was not included, since it has already been established to be negligible [25] for this system.

Within the Density Functional Theory [26–28], all calculations were performed with the software suite OpenMX [29], which self-consistently finds the eigenvalues and eigenfunctions of the Kohn–Sham [30] equations for the systems under study using fully relativistic norm-conserving pseudopotentials, and pseudoatomic orbitals (PAOs) for the expansion of the wave function; both contributed by Ozaki and Kino [31,32]. The PAO basis functions were specified by Co6.0-s2p2d1, Mn8.0-s2p2d1, Al7.0-s2p2d1, and Au7.0-s2p2d1, where, e.g., Co is the atomic symbol, 6.0 is the cutoff radius (Bohr) according to the confinement scheme utilized [31,32], and s2p2d1 means the employment of two primitive orbitals for each s and p orbital and one for the d orbital. We used the Perdew–Burke–Ernzerhof [33] generalized gradient approximation (GGA) for the exchange and correlation. While it is usually found that a Coulomb potential (GGA+U, e.g., Ref. [34]) is needed for the correct description of the d-bands of cobalt and manganese in these kind of alloys, Kandpal et al. [17] report that, for Co<sub>2</sub>MnAl, it is actually better the prediction of its experimental total magnetic moment if no orbital-dependent Coulomb potentials are added. Hence, we performed our calculations without “U” and, indeed, found a  $m_t = 4.02 \mu_B$  for the bulk, in excellent agreement with the experimental values of  $4.01 \pm 0.05 \mu_B$  (Ref. [3]) and  $4.07 \mu_B$  (Ref. [35]).

### 3. Discussion of results

Fig. 1(f) shows our optimization of the distance  $h$  between the two slabs that make up our models, the optimal distances – used for the rest of the calculations – were found to be of  $h_{\text{Co}_2\text{-t}}^0 = 2.37$  Å and  $h_{\text{MnAl-t}}^0 = 2.31$  Å; these rather large separations suggest a low chemical interaction between the two materials. Spin-resolved total densities of states (DOS) for the layers closest to the interface ( $L_0$ ,  $L_{-1}$ , and  $L_{-2}$ ) are shown in Fig. 2, and the corresponding ones for the free surfaces and the bulk are also included for comparison. We verified that the DOS for the most bulk-like layers ( $L_3$ ,  $L_{-5}$ ,  $L_{-6}$  and  $L_{-7}$ , not shown in Fig. 2), as much for the interfaces as for the free surfaces, are practically identical to those for the bulks; this probes that we have chosen enough atomic layers (or vacuum, for the free surfaces) so as to decouple adjacent supercells. In general, layer  $L_0$  (Au) is very alike in both models, but a critical difference appears at  $E_F$ : while for Co<sub>2</sub>-t there is an increase of the spin down (DW) DOS, which implies a spin polarization (SP) of  $-31.5\%$  (see arrow in the top left panel of Fig. 2), this feature does not appear in MnAl-t (which presents a SP of only  $+2.1\%$  at  $E_F$ , much closer to the SP=0% of pure gold). As to the DOS of the gold free surface and the bulk, they present strong differences with that of the gold at the interface (for both models): in the free surface, electrons of both spin channels migrate symmetrically towards  $E_F$ , while in the interfaces the electron populations tend to reorganize away from the  $E_F$  and asymmetrically. These differences, however, do not imply a significant magnetization of the gold (as can be seen in Table 1). At  $L_{-1}$ , a shift of the up-electrons away from  $E_F$  is clearly observed for Co and Mn atoms of both models, while down-electrons of Co atoms for Co<sub>2</sub>-t shift towards the Fermi energy. As a consequence, for Co<sub>2</sub>-t at  $L_{-1}$ , there is a SP=  $-70.4\%$  at  $E_F$  (see

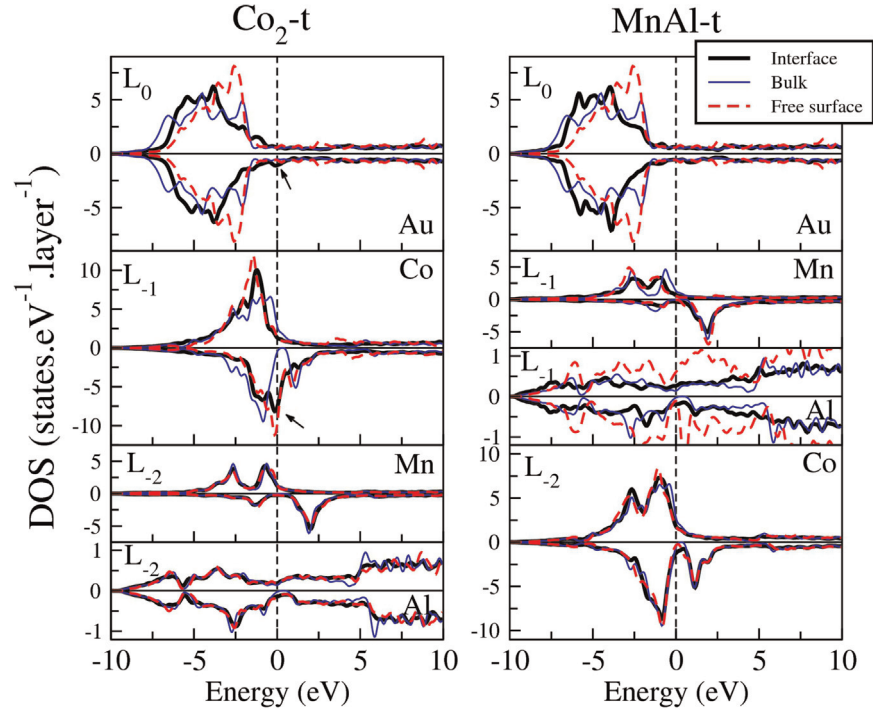


Fig. 2. Densities of states per layer for the two models (Co<sub>2</sub>-t and MnAl-t).

**Table 1**

Layer-resolved, atom type averaged charge and magnetic moment (MM) analysis for the two models of the interface. All values are in atomic units.

		Co <sub>2</sub> -t interface (free surface)						
		L <sub>-6</sub>	L <sub>-5</sub>	L <sub>-2</sub>	L <sub>-1</sub>	L <sub>0</sub>	L <sub>1</sub>	L <sub>3</sub>
Co	UP	–	7.98(7.98)	–	8.20(8.36)	–	–	–
	DW	–	7.32(7.32)	–	6.88(6.79)	–	–	–
	TOTAL	–	15.30(15.30)	–	15.08(15.15)	–	–	–
	MM	–	0.66(0.66)	–	1.32(1.57)	–	–	–
Mn	UP	8.86(8.85)	–	8.94(8.90)	–	–	–	–
	DW	5.77(5.78)	–	5.69(5.74)	–	–	–	–
	TOTAL	14.63(14.63)	–	14.63(14.64)	–	–	–	–
	MM	3.09(3.07)	–	3.25(3.16)	–	–	–	–
Al	UP	1.24(1.23)	–	1.26(1.22)	–	–	–	–
	DW	1.54(1.55)	–	1.57(1.55)	–	–	–	–
	TOTAL	2.78(2.78)	–	2.83(2.77)	–	–	–	–
	MM	–0.30(–0.32)	–	–0.31(–0.33)	–	–	–	–
Au	UP	–	–	–	–	8.53(8.52)	8.50(8.49)	8.50(8.50)
	DW	–	–	–	–	8.52(8.52)	8.51(8.49)	8.50(8.50)
	TOTAL	–	–	–	–	17.05(17.04)	17.01(16.98)	17.00(17.00)
	MM	–	–	–	–	0.01(0.00)	–0.01(0.00)	0.00(0.00)
		MnAl-t interface (free surface)						
		L <sub>-7</sub>	L <sub>-6</sub>	L <sub>-2</sub>	L <sub>-1</sub>	L <sub>0</sub>	L <sub>1</sub>	L <sub>3</sub>
Co	UP	–	7.97(7.97)	8.10(8.07)	–	–	–	–
	DW	–	7.32(7.33)	7.21(7.22)	–	–	–	–
	TOTAL	–	15.30(15.30)	15.31(15.29)	–	–	–	–
	MM	–	0.65(0.64)	0.89(0.85)	–	–	–	–
Mn	UP	8.86(8.87)	–	–	9.19(9.35)	–	–	–
	DW	5.76(5.76)	–	–	5.42(5.20)	–	–	–
	TOTAL	14.62(14.63)	–	–	14.61(14.55)	–	–	–
	MM	3.10(3.11)	–	–	3.77(4.15)	–	–	–
Al	UP	1.24(1.23)	–	–	1.30(1.46)	–	–	–
	DW	1.54(1.54)	–	–	1.54(1.71)	–	–	–
	TOTAL	2.78(2.77)	–	–	2.84(3.17)	–	–	–
	MM	–0.31(–0.31)	–	–	–0.25(–0.25)	–	–	–
Au	UP	–	–	–	–	8.56(8.52)	8.50(8.49)	8.50(8.50)
	DW	–	–	–	–	8.56(8.52)	8.50(8.49)	8.50(8.50)
	TOTAL	–	–	–	–	17.12(17.04)	17.00(16.98)	17.00(17.00)
	MM	–	–	–	–	0.00(0.00)	0.00(0.00)	0.00(0.00)

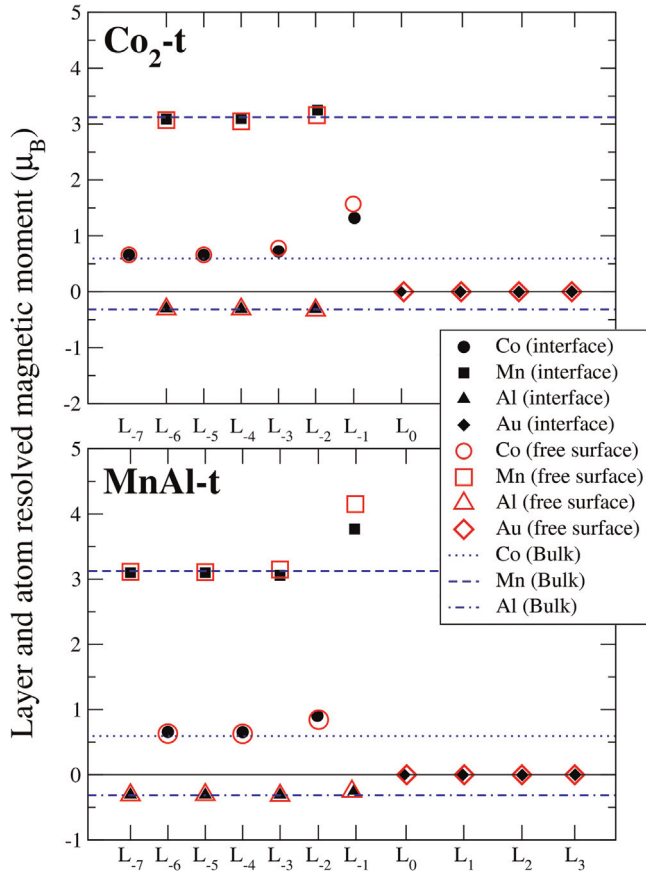


Fig. 3. Layered and atom resolved magnetic moment for the interface and the free surface for the two models ( $\text{Co}_2\text{-t}$  and  $\text{MnAl-t}$ ).

arrow in Fig. 2), while the value for the bulk is +68.3%, i.e., there is a full inversion of the sign of SP. This feature is distinctive of  $\text{Co}_2\text{-t}$ , since  $\text{MnAl-t}$  at  $L_{-1}$  shows a positive SP = +27.7%. Hence, the interface quenches the SP for  $\text{MnAl-t}$ , while it inverts it for  $\text{Co}_2\text{-t}$ . This strongly suggests that important differences in transport properties for the two different terminations of the interface are to be expected. It is seen that DOS at  $L_{-2}$ , of the interfaces and of the free surfaces, already mimic almost exactly those of the bulk.

In Fig. 3 we present the atom and layer resolved magnetic moments for the interface and the free surface, while Table 1 allows a detailed analysis of the charges (UP, DW, and total) and magnetic moments (MM) for selected layers: most bulk-like ( $L_{-7}$ ,  $L_{-6}$ ,  $L_{-5}$ , and  $L_3$ ) and those at the interface ( $L_{-2}$ ,  $L_{-1}$ ,  $L_0$ , and  $L_1$ ). For  $\text{Co}_2\text{-t}$  (interface and free surface) the total charge of cobalt atoms at  $L_{-1}$  is slightly lower than at  $L_{-5}$ , while the magnetic moment is greater by a factor of more than 2. This can be explained by a migration of DW-electrons partially to the UP channel of the same cobalt atoms, and partially to the gold atoms at  $L_0$  and the aluminum atoms at  $L_{-2}$  (for the interface). Also at  $L_{-2}$ , it is seen that Mn atoms increase their magnetization by a redistribution of their electrons, since their total charge remains constant. Both the gold of the interface and the gold free surface have a slight gain of charge at  $L_0$  ( $\sim 0.05$  au), practically without magnetization: this indicates that the redistribution of charge at the gold side of the interface must mostly be due to the break of symmetry, rather than the interaction with  $\text{Co}_2\text{MnAl}$ . In the  $\text{MnAl-t}$  interface, there is also a sensible increase of the magnetization at the interface, with almost no change of the total charges at  $L_{-1}$  and  $L_{-2}$  (compared to the bulk-like layers). In contrast, in the  $\text{MnAl-t}$  free surface, the Al atoms show a sensible increase of their total charge (3.17 au, compared to 2.84 au of the interface and

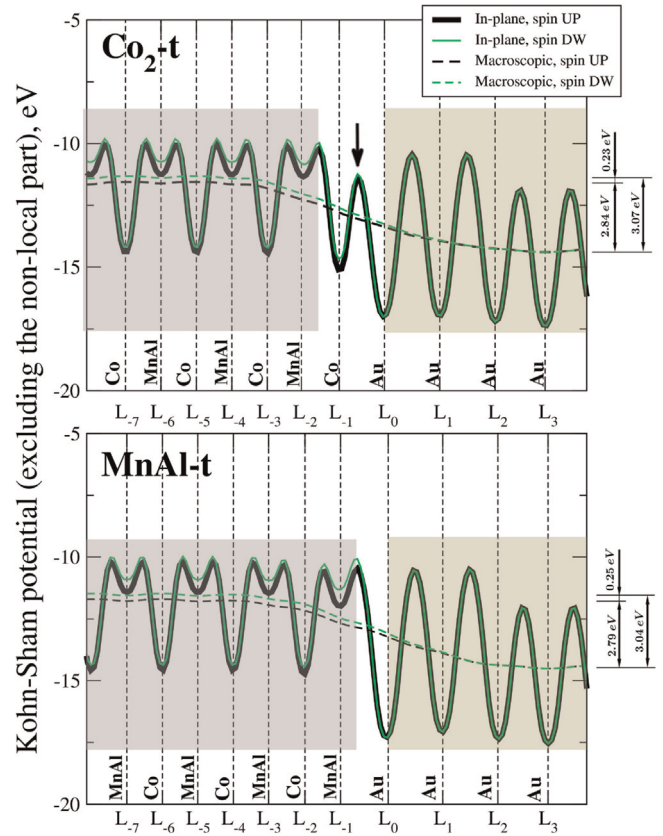


Fig. 4. Kohn-Sham potential (excluding the non-local part) along the interface for the two models ( $\text{Co}_2\text{-t}$  and  $\text{MnAl-t}$ ).

2.78 au of the most bulk-like layers): this difference is due to the absence of the gold which, when present, gets negatively charged mostly due to migration of electrons from the Al atoms.

Fig. 4 shows the in-plane potential, which results from integrating throughout the  $yz$  planes (i.e., planes parallel to the interface) and the so called “macroscopic” potential: an average along  $x$  (i.e., a smoothed version) of the former [36,37]. The potential shown is that of Kohn-Sham except for the non-local potential (which due to its non-locality cannot simply be added to the rest; and is of importance only close to the atomic cores). This potential could account for the 0.25 eV of difference between channels UP and DW which are otherwise practically identical. It is to be noticed that for  $\text{Co}_2\text{-t}$ , there is a peak of the in-plane potential just at the interface, between the last Co plane and the first Au plane (see arrow in Fig. 4), which is absent in the  $\text{MnAl-t}$  interface. It is important to note that while this peak is “hidden” in the macroscopic potential due to the smoothing action of averaging along the  $x$ -direction, it is indeed what electrons will “see” when traveling through the interface. We hypothesize that this difference of the in-plane potential of  $\text{Co}_2\text{-t}$  and  $\text{MnAl-t}$  interfaces might be of relevance to the electronic transport through the interface. For both models the contact potential between the Heusler alloy and the gold is  $\approx 3.05$  eV, with the  $\text{Co}_2\text{MnAl}$  side positive respect to the gold: this suggests that the work function of the Heusler ( $W_{\text{Heusler}}$ ) alloy is lower than that of gold (a rigorous determination of  $W_{\text{Heusler}}$  implies calculations [38,39] beyond the scope of the present work).

#### 4. Conclusions

We studied electronic and magnetic properties of the interface  $\text{Co}_2\text{MnAl}/\text{Au}$ , finding that the Heusler termination (either



Co<sub>2</sub>-t or MnAl-t) is crucial to the definition of the electronic properties at the interface both quantitatively and qualitatively and so, presumably, of high importance regarding applications of this material in spintronic devices. A greater spin polarization at E<sub>F</sub> suggests the Co<sub>2</sub> termination should be more attractive as a spin injector. However, a noticeable difference of the morphology of the in-plane potential for the Co<sub>2</sub>-t and MnAl-t interfaces, just at the transition region, might affect transport in a non-negligible way. Thus it is clear that non-equilibrium spin-resolved electronic transport calculations of these interfaces are necessary to resolve which one would be more suitable for spintronic applications. Finally, it is worth mentioning that relative positions of the slabs in the yz plane other than the one chosen here (such as top site) should be of high interest for further understanding the physics of this interface.

## Acknowledgments

This work was supported by the Consejo Nacional de Investigaciones Científicas y Técnicas (Argentina), and the Facultad de Ingeniería, Universidad Nacional de Entre Ríos (Argentina). The work of the developers of VESTA code [40], utilized in this paper, is also acknowledged.

## References

- [1] R.A. de Groot, F.M. Mueller, P.G. van Engen, K.H.J. Buschow, *Phys. Rev. Lett.* 50 (1983) 2024.
- [2] R.A. de Groot, F.M. Mueller, P.G. van Engen, K.H.J. Buschow, *J. Appl. Phys.* 55 (1984) 2151.
- [3] J. Kübler, A.R. Williams, C.B. Sommers, *Phys. Rev. B* 28 (1983) 1745.
- [4] I. Galanakis, P.H. Dederichs, N. Papanikolaou, *Phys. Rev. B* 66 (2002) 174429.
- [5] G.H. Fecher, H.C. Kandpal, S. Wurmehl, C. Felser, G. Schönhense, *J. Appl. Phys.* 99 (2006) 08J106.
- [6] Y. Miura, K. Nagao, M. Shirai, *Phys. Rev. B* 69 (2004) 144413.
- [7] I. Žutić, J. Fabian, S. Das Sarma, *Rev. Mod. Phys.* 76 (2004) 323.
- [8] C. Felser, G.H. Fecher, B. Balke, *Angew. Chem. (Int. Ed.)* 46 (2007) 668.
- [9] Aniruddha Deb, M. Itou, Y. Sakurai, N. Hiraoka, N. Sakai, *Phys. Rev. B* 63 (2001) 064409.
- [10] S. Kämmerer, A. Thomas, A. Hütten, G. Reiss, *Appl. Phys. Lett.* 85 (2004) 79.
- [11] Y. Sakuraba, M. Hattori, M. Oogane, Y. Ando, H. Kato, A. Sakuma, T. Miyazaki, H. Kubota, *Appl. Phys. Lett.* 88 (2006) 192508.
- [12] X.Y. Dong, C. Adelmann, J.Q. Xie, C.J. Palmstrom, X. Lou, J. Strand, P.A. Crowell, J. P. Barnes, A.K. Petford-Long, *Appl. Phys. Lett.* 86 (2005) 102107.
- [13] P.J. Webster, *J. Phys. Chem. Solids* 32 (1971) 1221.
- [14] K.H.J. Buschow, P.G. van Engen, *J. Magn. Magn. Mater.* 25 (1981) 90.
- [15] S. Plogmann, T. Schlathöller, J. Braun, M. Neumann, Y.M. Yarmoshenko, M. V. Yablonskikh, E.I. Shreder, E.Z. Kurmaev, A. Wrona, A. S'lebarski, *Phys. Rev. B* 60 (1999) 6428–6438.
- [16] J. Kübler, G.H. Fecher, C. Felser, *Phys. Rev. B* 76 (2007) 024414.
- [17] H.C. Kandpal, G.H. Fecher, C. Felser, *J. Phys. D: Appl. Phys.* 40 (2007) 1507–1523.
- [18] X. Jia, W. Yang, M. Qin, L. Wang, *J. Phys. D: Appl. Phys.* 41 (2008) 085004.
- [19] V. Jung, G.H. Fecher, B. Balke, V. Ksenofontov, C. Felser, *J. Phys. D: Appl. Phys.* 82 (2009) 084007.
- [20] S. Chadov, T. Graf, K. Chadova, X. Dai, F. Casper, G.H. Fecher, C. Felser, *Phys. Rev. Lett.* 107 (2011) 047202.
- [21] S. Isber, Y.J. Park, J.S. Moodera, D. Heiman, *J. Appl. Phys.* 103 (2013) 07D713.
- [22] Y. Si-Peng, S. Chao, Z. Hou-Zhi, L. Qi, W. Li-Guo, M. Kang-Kang, Z. Jian-Hua, *Chin. Phys. B* 22 (2013) 047202.
- [23] Y. Sakuraba, K. Izumi, T. Iwase, S. Bosu, K. Saito, K. Takanashi, Y. Miura, K. Futatsukawa, K. Abe, M. Shirai, *Appl. Phys. Lett.* 82 (2010) 094444.
- [24] B. Särk, P. Krüger, J. Pollmann, *Phys. Rev. B* 81 (2010) 035321.
- [25] I. Galanakis, *Phys. Rev. B* 71 (2005) 012413.
- [26] L. Thomas, *Proc. Camb. Philos. Soc.* 23 (1927) 542.
- [27] E. Fermi, *Z. Phys.* 48 (1928) 73.
- [28] P. Hohenberg, W. Kohn, *Phys. Rev.* 136 (1964) B864.
- [29] T. Ozaki, K. Nishio, H. Kino, *Phys. Rev. B* 81 (2010) 035116.
- [30] W. Kohn, L. Sham, *Phys. Rev.* 140 (1965) A1133.
- [31] T. Ozaki, *Phys. Rev. B* 67 (2003) 155108.
- [32] T. Ozaki, H. Kino, *Phys. Rev. B* 69 (2004) 195113.
- [33] J.P. Perdew, K. Burke, M. Ernzerhof, *Phys. Rev. Lett.* 77 (1996) 3865.
- [34] J. Chen, X. Wu, A. Selloni, *Phys. Rev. B* 83 (2011) 245204.
- [35] R.Y. Umetsu, K. Kobayashi, A. Fujita, R. Kainuma, K. Ishida, *J. Appl. Phys.* 103 (2008) 07D718.
- [36] M. Peressi, N. Binggeli, A. Baldereschi, *J. Phys. D: Appl. Phys.* 31 (1998) 1273–1299.
- [37] J.P. Velev, P.A. Dowben, E.Y. Tsybmal, S.J. Jenkins, A.N. Caruso, *Surf. Sci. Rep.* 63 (2008) 400–425.
- [38] C.J. Fall, N. Binggeli, A. Baldereschi, *J. Phys.: Condens. Matter* 11 (1999) 2689–2696.
- [39] C.J. Fall, C. Ab Initio Study of the Work Functions of Elemental Metal Crystals (Ph.D. thesis, No. 1955), Department of Physics, Ecole Polytechnique Federale De Lausanne, Lausanne, Switzerland, 1999.
- [40] K. Momma, F. Izumi, *J. Appl. Crystallogr.* 44 (2011) 1272–1276.